(14) (a) For the purpose of π-orbital classification, all molecules treated (1–8, planar as well as pyramidal forms) are regarded to have C_{2v} symmetry. (b) spd means here, as usual, inclusion of the five 3d orbitals on phosphorus in the atomic orbital basis set otherwise consisting only of the valence s and p orbitals of all atoms involved (i.e., the sp basis). In extending the CNDO/S procedure, explicit provision was made to avoid the over-emphasis of the importance of 3d orbitals known from the usual CNDO/2 method. For full details, see ref 9. (c) According to current ideas of conjugative effects in five-membered heterocycles as furane, thiophene, and pyrrole, the heteroatom lone pair (n) orbital energy is expected to be appreciably shifted in these systems relative to the corresponding n orbital energy in suitably chosen saturated reference compounds or in the respective conjugatively decoupled species as used here (for a confirmation of these ideas in the case of pyrrole, see Figure 1 of text). In addition, the idea that properties of the phosphorus lone pair (e.g., its energy) in the neighborhood of attached π systems are directly indicative of its involvement in π conjugation is very common in phosphorus chemistry. Against this backdrop, we interpreted—in a preceding preliminary (in sense that the calculations of the present paper were neither available nor possible) publication[32]—our photoelectron spectroscopic observation that the n orbital energy in 1-phenylphosphole is not noticeably influenced by the attached cis-butadiene system as evidence for the "nonaromaticity" of phospholes. In view of the new theoretical insight into conjugated effects in phospholes gained in the present paper (it is essential in this context that the n orbital energy stays constant due to combined $n\pi$ and $n\pi^*$ effects), we may tentatively reinterpret the same experimental observation now as evidence for an "aromatic" nature of phospholes. As in this context, it must be stressed, however, that the present calculations do present the first clear-cut and direct theoretical evidence for an "aromatic" pyramidal phosphole ground state previously not available and, on the other hand, one should not forget that till now no clear experimental answer has become available to whether phospholes in their ground state conformation are "aromatic" or "nonaromatic" systems.

(15) The orbital plots show the CNDO/S density after renormalization by the Löwdin transformation (including diatomic overlap).[16] This ZDO orbital renormalization procedure was previously used on the CNDO/2 (INDO) level by several authors.[17-20] As previously shown[21] only the renormalized orbitals produce electron densities with correct nodal properties.

(16) P. O. Löwdin, J. Chem. Phys., 18, 365 (1950).

(17) C. Giesner-Prettre and A. Pullman, Theor. Chim. Acta, 11, 159(1968).

(18) D. D. Shillady, F. P. Billingsley, and J. E. Bloor, Theor. Chim. Acta, 21, 1 (1971).

(19) D. B. Boyd, J. Amer. Chem. Soc., 94, 64 (1972).

(20) J. W. McIver, P. Coppens, and D. Nowak, Chem. Phys. Lett., 11, 82 (1971).

(21) H. L. Hase, H. Meyer, and A. Schweig, Z. Naturforsch. A, 29, 361 (1974).

(22) For the plot program used, see: (a) H. Hahn and J. Radloff, Elektron. Rechenanl., 14, 128 (1972); (b) H. L. Hase, A. Schweig, H. Hahn, and J. Radloff, Tetrahedron, 29, 475 (1973); (c) ibid., 29, 469 (1973).

(23) W. Egan, R. Tang, G. Zon, and K. Mislow, J. Am. Chem. Soc., 92, 1442 (1970).

(24) D. A. Brown, J. Chem. Soc., 929 (1962).

(25) J. Del Bene and H. H. Jaffé, J. Chem. Phys., 48, 1807 (1968).

(26) J. Del Bene and H. H. Jaffé, J. Chem. Phys., 48, 4050 (1968).

(27) The role of d orbitals on phosphorus has also been recognized elsewhere: G. Kaufmann and F. Mathey, Phosphorus, 4, 231 (1974).

(28) For the synthesis of these compounds, see: (a) F. Mathey and R. Mankowski-Favelier, Bull. Soc. Chim. Fr., 4433 (1970); (b) J. Org. Magn. Reson., 4, 171 (1972); (c) F. Mathey, Tetrahedron, 28, 4171 (1972).

(29) J. H. Hillier and V. R. Saunders, J. Chem. Soc., Faraday Trans. 2, 66, 2401 (1970).

(30) S. Elbel, H. Bergmann, and W. Ensslin, J. Chem. Soc., Faraday Trans. 2, 70, 555 (1974).

(31) H. Schmidt, A. Schweig, F. Mathey, and G. Müller, Tetrahedron, 31, 1287 (1975).

(32) W. Schäfer, A. Schweig, G. Märkl, H. Hauptmann, and F. Mathey, Angew. Chem., 85, 140 (1973); Angew. Chem., Int. Ed. Engl., 12, 145 (1973).

(33) Ion states calculated on the base of Koopmans' theorem: T. Koopmans, Physica, 1, 104 (1934).

(34) G. Lauer, K. W. Schulte, and A. Schweig, Chem. Phys. Lett., 32, 163 (1975).

(35) G. Lauer, W. Schäfer, and A. Schweig, Chem. Phys. Lett., 33, 312 (1975).

(36) E. Heilbronner, R. Gleiter, H. Hopf, V. Hornung, and A. de Meijere, Helv. Chim. Acta, 54, 783 (1971).

(37) C. Batich, P. Bischoff, and Heilbronner, J. Electron Spectrosc. Relat. Phenom., 1, 333 (1972–1973).

(38) P. Bischoff, J. A. Hashmall, E. Heilbronner, and V. Hornung, Helv. Chim. Acta, 52, 1745 (1969).

Mechanisms of Ligand Association in Complexes of the Type RML3+X- (M = Ni, Pd, Pt). I. Mechanistic Aspects of Nuclear Magnetic Resonance Line Shape Analysis for Intermolecular Exchange in Non-First-Order Multispin Systems

P. Meakin,* A. D. English,* and J. P. Jesson*

Contribution No. 2262 from the Central Research and Development Department, Experimental Station, E.I. du Pont de Nemours and Company, Wilmington, Delaware 19898. Received April 18, 1975

Abstract: General computer programs applicable to intermolecular exchange in non-first-order spin systems have been developed. Their scope and application is illustrated with reference to the equilibrium $HPd[P(C_2H_5)_3]_3^+ + P(C_2H_5)_3 \rightleftharpoons HPd[P(C_2H_5)_3]_4^+$. In this case four separate rate processes can be considered, k_1, k_{-1}, k_m (the rate of intramolecular rearrangement in HML_4^+), and k_m' (the rate of intramolecular rearrangement in HML_3^+). The computer programs can be applied to a wide range of combinations of simultaneously occurring intermolecular and intramolecular processes. Permutational analyses have been carried out for the intermolecular case which are an extension of those we have developed earlier for intramolecular rearrangement. The approach enables one to extract detailed mechanistic information concerning the mode of ligand attack and the site occupied by the attacking ligand in the five-coordinate intermediate. It also allows the generation of linear combinations of permutational sets, for use in the line shape calculations where competing rate processes are occurring at comparable rates. This can lead to a quantitative estimate of the ratio of the two rates, e.g., k_{-1}/k_m.

The application of detailed NMR line shape analyses to the determination of both rates and mechanisms for transition metal complexes undergoing intramolecular exchange is well established. In contrast, relatively little work of this type has been carried out for intermolecular exchange processes. General computer programs which can handle non-first-order multispin systems undergoing intramolecular exchange have been available for some years.[1-4] Most NMR line shape calculations for intermolecular exchange have been restricted to first-order systems where existing computer programs for nonmutual intermolecular exchange can be used directly or with slight modification. In some in-

stances,[5,6] programs have been written to analyze the line shapes associated with a particular problem involving intermolecular exchange in non-first-order spin systems. Only very recently have general computer programs applicable to a wide range of intermolecular exchange processes in non-first-order spin systems been developed. This paper describes new general programs of this type and shows how they may be used to extract detailed kinetic and mechanistic information for a given reaction. The approach is illustrated with respect to the equilibrium.

$$HPd[P(C_2H_5)_3]_3^+ + P(C_2H_5)_3 \underset{k_{-1}}{\overset{k_1}{\rightleftharpoons}} HPd[P(C_2H_5)_3]_4^+ \quad (1)$$
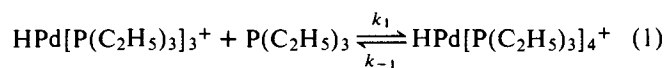
The line shape programs include both the effects of the intermolecular exchange shown in eq 1 and the effects of intramolecular rearrangement in both HML_3^+ and HML_4^+.[7]

Mechanistic Analysis

The number of distinguishable types of NMR line shape behavior, and the permutations corresponding to them, can be determined using the same techniques that were introduced earlier for determining the "basic permutational sets" for mutual exchange.[2,8] Since the intermolecular exchange process is clearly ligand catalyzed (vide infra), only processess of this type will be considered. Our initial discussion is confined to the case where ligand exchange occurs in a concerted process. The overall effect of the exchange can be described in terms of permutations involving both free and complexed ligand. The numbering scheme used in the permutational analysis is shown in configuration 1. The hy-

L_2   ·L_4
|
H——M——L_1
|
L_3

1
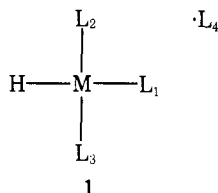
dride ligand is not labeled since it is not directly involved in the exchange process. The system shown in configuration 1 is invariant under the permutations

$$g_1 = E = (1) (2) (3) (4) \text{ and}$$

$$g_2 = \sigma = (1) (23) (4)$$

Starting with the 4! = 24 possible permutations for the phosphorus nuclei in the HML_3^+/L system and using the permutational group $G = (g_1, g_2)$, seven basic sets can be generated using the procedures described in our earlier work.[2,8] The results obtained with a computer program described previously are given in Table I. In this case, the results could be written down by inspection but for more complex cases[9,10] a computer analysis is essential. Set VI is the identity set corresponding to NMR line shapes which are invariant to temperature and ligand concentration. Set V corresponds to mutual intramolecular exchange but this process could also be ligand catalyzed. Sets I–IV correspond to processes in which the free and complexed ligands are exchanged. Sets I and IA are the inverses of each other and must occur at the same rate by microscopic reversibility. Consequently, all of the permutations corresponding to sets I and IA must be included together at the same rate in the line shape calculations, reducing the seven basic sets to six possible types of NMR line shape behavior. Our computer program has been modified to group together basic sets and their inverses, in those cases where a set is not its own inverse. Set IV corresponds to processes in which complexed ligands L_2 and L_3 exchange with free ligand L_4. Li-

Table I. Basic Permutation Sets for the HML_3^+–L System

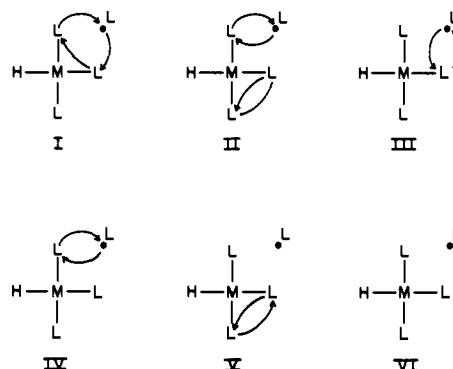| Label	Set	Equivalent Set
I	(1324)	(124) (3)
	(1234)	(134) (2)
IA	(1423)	(142) (3)
	(1432)	(143) (2)
II	(13) (24)	(1243)
	(12) (34)	(1342)
III	(14) (23)	(14) (2) (3)
IV	(1) (243)	(1) (24) (3)
	(1) (234)	(1) (34) (2)
V	(13) (2) (4)	(123) (4)
	(12) (3) (4)	(132) (4)
VI	(1) (2) (3) (4)	(1) (23) (4)

Figure 1. Schematic representation of the basic sets for the HML_3^+-L system undergoing ligand catalyzed exchange.

gand L_1 remains unique. Set III corresponds to processes in which L_1 is the only complexed ligand exchanging with free ligand. Sets (I, IA) and II correspond to processes in which all four ligand spins are eventually scrambled. Sets (VI ≡ E), V, IV, III, and ((I, IA) and II) all give different high temperature limit spectra so that a qualitative analysis can distinguish between all sets except I[11] and II. In most cases, sets I and II can be readily distinguished by a complete line shape analysis (vide infra). The sets I, II, III, IV, and V are represented diagramatically in Figure 1. (The figure depicts the overall permutational changes only; the arrows do not imply a particular physical motion; only one permutation from a given set is shown.)

The Effects of a Five-Coordinate Intermediate

If the actual reaction mechanism involves a five-coordinate intermediate with a very short preexchange lifetime, present in low concentrations, the time development of the spin density matrix in the HML_4^+ site can be ignored and the effect of the five-coordinate intermediate can be treated as a mechanism for permuting free and complexed ligands.[12] In this case, the NMR line shapes can be analyzed in terms of the basic sets for the HML_3^+-L system discussed above without including the HML_4^+ resonances explicitly. If the ligand L_1 remains unique throughout the exchange process (as is observed for $HPt[P(C_2H_5)_3]_3^+$),[7] the mechanism shown below is plausible, if the five-coordinate

L_2   H
| |
H——M——L_1 + L_4 ⇌ L_2——M⟨L_3
| | L_4
L_3   L_1

2
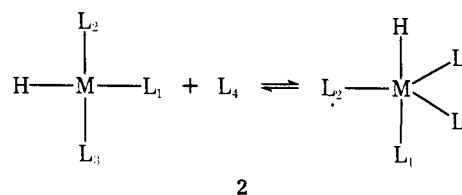
intermediate does not undergo mutual exchange before ligand dissociation. In this case, the associated NMR line

shapes can be analyzed using basic set IV $(E + IV)$.[13] When intramolecular exchange occurs in the five-coordinate intermediate, the linear combination

$$(1 - C)(E + IV) + (C/3)(I + II + III + V) \qquad (2)$$

must be used where C is the fraction of the five-coordinate intermediate molecules in which L_2, L_3, or L_4 have exchanged to the axial position before dissociation. Letting P_A represent the probability of the five-coordinate intermediate being in a state with L_1 axial, and P_B the probability of L_2, L_3, or L_4 being in an axial position, the effects of mutual exchange are given by

$$d/dt[P_A(t)] = -k_m P_A(t) + k_m P_B(t)/3 \qquad (3a)$$

$$d/dt[P_B(t)] = k_m P_A(t) - k_m P_B(t)/3 \qquad (3b)$$

where k_m is the rate of the mutual exchange process.

Equation 3 can be rewritten as

$$d/dt[P_A(t) + P_B(t)] = 0 \qquad (4a)$$

$$d/dt[P_A(t) - P_B(t)/3] =$$
$$-4k_m/3[P_A(t) - P_B(t)/3] \qquad (4b)$$

At time $t = 0$ (just after the HML_4^+ intermediate molecule has been formed) we have $P_A(0) = 1$, $P_B(0) = 0$ and these initial conditions with eq 4 give

$$P_A(t) = \tfrac{1}{4} + \tfrac{3}{4}e^{-(4k_m t/3)} \qquad (5a)$$

$$P_B(t) = \tfrac{3}{4}[1 - e^{-(4k_m t/3)}] \qquad (5b)$$

Since both the A and B states are dissociating with a rate constant k_{-1}, the probabilities $P_A(t)$ and $P_B(t)$ including the effects of both intramolecular exchange and ligand dissociation are given by

$$P_A(t) = \tfrac{1}{4}[1 + 3e^{-(4k_m t/3)}]e^{-k_{-1}t} \qquad (6a)$$

$$P_B(t) = \tfrac{3}{4}[1 - e^{-(4k_m t/3)}]e^{-k_{-1}t} \qquad (6b)$$

$$P_A(t) + P_B(t) = e^{-k_{-1}t} \qquad (6c)$$

The fraction of HML_4^+ molecules dissociating from a B state is given by

$$C = \int_0^\infty P_B(t)\, dt \Big/ \int_0^\infty [P_A(t) + P_B(t)]\, dt \qquad (7)$$

Equations 6 and 7 lead to the result

$$C = \tfrac{3}{4}\left[\frac{4k_m/3k_{-1}}{1 + 4k_m/3k_{-1}}\right] \qquad (8)$$

NMR line shapes, calculated using the linear combination of basic sets given by eq 2 and 8 for the HML_3^+-L system, are compared with those in which a small concentration of the HML_4^+ intermediate undergoing mutual exchange has been explicitly included, in a later section of this paper.

NMR Line Shape Calculations

The density matrix equations of motion used to calculate the NMR line shapes can be written as

$$\frac{d\rho_i}{dt} = 2\pi i[\rho_i, \mathcal{H}_i] + \left(\frac{d\rho_i}{dt}\right)_{exch} + \left(\frac{d\rho_i}{dt}\right)_{relax} \qquad (9)$$

where ρ_i is the mean spin density matrix and $\mathcal{H}_i$ is the high resolution NMR Hamiltonian for the ith species including the interaction with the rf field. $(d\rho_i/dt)_{relax}$ represents the effects of relaxation processes other than chemical exchange, the effects of magnetic field inhomogeneity, and the effects of incomplete noise decoupling in the case of the $^{31}P\{^1H\}$ spectra.

We use the simple form $(d\rho_i/dt)_{relax} = -\rho_i/T_{2i}$ for the density matrix elements one off-diagonal in I_z. T_{2i} is the ef-

fective relaxation time for the ith species which determines the line width in the absence of exchange. $(d\rho_i/dt)_{exch}$ is the exchange contribution for the ith species. The exchange contributions to the density matrix equations for intermolecular processes have been given by Kaplan[14] and Alexander.[15] For the HML_3^+-L system, these are

$$\left(\frac{d\rho_A}{dt}\right)_{exch} = \sum_j \frac{1}{\tau_{Aj}} \{Tr_B[P_j(\rho_A \otimes \rho_B)P_j^{-1}] - \rho_A\} \qquad (10a)$$

$$\left(\frac{d\rho_B}{dt}\right)_{exch} = \sum_j \frac{1}{\tau_{Bj}} \{Tr_A[P_j(\rho_A \otimes \rho_B)P_j^{-1}] - \rho_B\} \qquad (10b)$$

where ρ_A and ρ_B are the spin density matrices for HML_3^+ and L, respectively, and P_j is the matrix representation of the jth permutation. τ_{Aj} and τ_{Bj} are the preexchange lifetimes for HML_3^+ and L with respect to the jth process. The symbol $\otimes$ implies a direct product of the matrix representations. The symbols Tr_A and Tr_B indicate summation over all elements diagonal in the A and B indices, respectively. It has been assumed that ρ_A and ρ_B have been normalized such that $Tr\rho_A = 1$ and $Tr\rho_B = 1$. For the HML_4^+-HML_3^+-L system, the appropriate exchange contributions are

$$\left(\frac{d\rho_A}{dt}\right)_{exch} = \sum_j 1/\tau_{Aj}\{Tr_{Bj}(\rho_C) - \rho_A\} \qquad (11a)$$

$$\left(\frac{d\rho_B}{dt}\right)_{exch} = \sum_j 1/\tau_{Bj}\{Tr_{Aj}(\rho_C) - \rho_B\} \qquad (11b)$$

$$\left(\frac{d\rho_C}{dt}\right)_{exch} = \sum_j 1/\tau_{Cj}\{\rho_A \otimes \rho_B - \rho_C\} +$$
$$\sum_k 1/\tau_{Ck}\{P_k\rho_C P_k^{-1} - \rho_C\} \qquad (11c)$$

where ρ_C is the spin density matrix for HML_4^+ and the P_k are the permutations describing the kth mutual exchange process in the five-coordinate intermediate. In eq 11a, $Tr_{Bj}(\rho_C)$ indicates summation over all elements of ρ_C diagonal in indices for the spins which exchange with spins in B during the jth process. A basis consisting of simple products of the eigenvectors of the z components of nuclear spin is implied. $Tr_{Aj}(\rho_C)$ is to be interpreted similarly. The index j indicates which ligands in a labeled HML_4^+ molecule are exchanged with the ligands in labeled HML_3^+ and L molecules. For example, if the HML_4^+ is labeled as shown in 3,

3
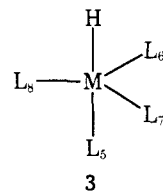
HML_3 and L are labeled as shown in 1, and if the exchange mechanism is that given in 2, the exchange processes E_j ($j = 1$-6) must be included together in the line shape analysis above.

$$E_1 = (15) \quad (26) \quad (37) \quad (48)$$
$$E_2 = (15) \quad (26) \quad (38) \quad (47)$$
$$E_3 = (15) \quad (27) \quad (38) \quad (46)$$
$$E_4 = (15) \quad (27) \quad (36) \quad (48)$$
$$E_5 = (15) \quad (28) \quad (37) \quad (46)$$
$$E_6 = (15) \quad (28) \quad (36) \quad (47)$$

Since intramolecular mutual exchange is observed in some cases for HML_3^+, $(HNi[P(C_2H_5)_3]_3^+)$,[7] as well as HML_4^+, eq 11a must be extended to

$$\left(\frac{d\rho_A}{dt}\right)_{\text{exch}} = \sum_j 1/\tau_{Aj}\{Tr_{Bj}(\rho_C) - \rho_A\} +$$

$$\sum_l 1/\tau_{Al}\{P_l\rho_A P_l - \rho_A\} \quad (11d)$$

to include the effects of exchange in HML_3^+. P_l is the matrix representation for the lth mutual exchange permutation in HML_3^+ and τ_{Al} is the preexchange lifetime for P_l. In the case where the central metal has isotopes with $I = 0$ and $I = \frac{1}{2}$ (Pt),[7] there are three HML_3^+ sites corresponding to: (1) the molecules with M isotopes of spin zero, (2) the molecules with M isotopes with $I = \frac{1}{2}$ in spin state α, (3) the molecules with M isotopes with $I = \frac{1}{2}$ in spin state β. Equation 10 can then be generalized to give

$$\left(\frac{d\rho_{Ak}}{dt}\right)_{\text{exch}} = \sum_j 1/\tau_{Aj}\{Tr_B[P_j(\rho_{Ak}\otimes\rho_B)P_j^{-1}] - \rho_{Ak}\}$$

$$(12a)$$

$$\left(\frac{d\rho_B}{dt}\right)_{\text{exch}} = \sum_j \sum_k 1/\tau_{Bjk} \times$$

$$\{Tr_{Ak}[P_j(\rho_{Ak}\otimes\rho_B)P_j^{-1}] - \rho_B\} \quad (12b)$$

where the subscript k refers to the kth HML_3^+ site.

The density matrix equations of motion are set up initially in the basis consisting of the simple products of the eigenvectors of the z components of angular momentum for the individual spins using the permutation of the indices method of Kaplan and Fraenkel.[16] This method simplifies considerably the application of eq 10–12 to the calculation of NMR line shapes. The equations of motion are then transformed to the basis in which the high resolution NMR Hamiltonians and the Liouville operators are diagonal using the transformations obtained from a numerical diagonalization of the high resolution NMR Hamiltonians. This basis has the advantage that there is a 1:1 correspondence between the density matrix elements one off diagonal in I_z and the NMR transitions. It is found that, if the group of the high resolution NMR Hamiltonian is Abelian, and if the exchange process has the full symmetry of this group, the density matrix equations of motion do not connect the density matrix elements corresponding to allowed transitions to those corresponding to forbidden, zero intensity, transitions. Consequently, the dimension of the coupled linear equations which must be solved to calculate the NMR line shapes is reduced just as in the mutual exchange case.[2] This basis also has the advantage that several approximations[17,18] can be used in cases where the spin system is too large for a complete line shape analysis. These approximate methods cannot be applied in the original spin product basis. Approximations were not required in the present work. The transformation of the density matrix equations of motion is discussed in more detail in the appendix. The final expression for the NMR line shapes which can be obtained by standard methods is of the form[18]

$$I(\omega) = -Re\{P^- \cdot \left[\sum_i X_i + R - iL(\omega)\right]^{-1} \cdot \sigma^-\} \quad (13)$$

where R is the relaxation matrix and L is the Liouville operator in composite Liouville space.[19] σ^- is a vector containing the elements of the transition operators σ_i^- given by

$$\sigma_i^- = \sum_j \gamma_{ij}I_{ij}^-/N_i \quad (14)$$

where γ_{ij} is the magnetogyric ratio for the jth spin in the ith species and I_{ij}^- is the corresponding spin lowering operator. N_i is the dimension of the spin space for the ith species given by $N_i = 2^{n_i}$ where n_i is the number of spins (of $\frac{1}{2}$) for the ith species. P^- is a similar vector containing the ele-
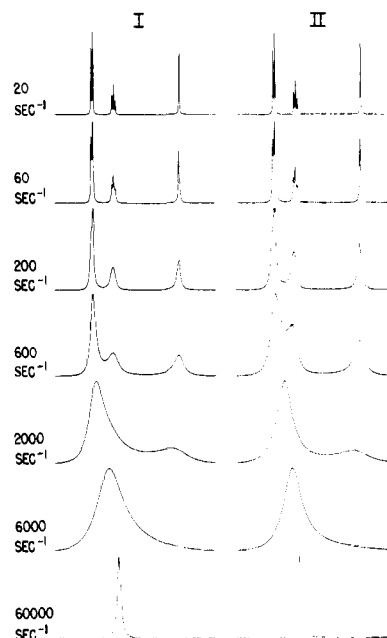

Figure 2. NMR line shapes calculated to simulate the $^{31}P\{^1H\}$ spectra for an HML_3^+-L system undergoing intermolecular exchange processes corresponding to basic sets I and II. (The slow exchange limit spectra in Figures 2-7 correspond to that observed for $HPd[P(C_2H_5)_3]_3^+$-$P(C_2H_5)_3$ in acetone.)[7]

ments of the operators P_i given by

$$P_i^- = \sum_j C_i\gamma_{ij}I_{ij}^- \quad (15)$$

where C_i is the concentration of the ith species.

Equation 13 is solved using the numerical techniques developed by Gordon and McGinnis,[20] Binsch,[1] and Schirmer, Noggle, and Gaines.[21] For intermolecular exchange, all of the off-diagonal density matrix elements corresponding to the allowed transitions for a particular nuclear species are connnected by the elements of the exchange matrix χ, and no symmetry factoring, apart from the separation of density matrix elements corresponding to allowed transitions from those corresponding to forbidden transitions, is possible. X factoring[2] is still possible however. Because of the much less extensive factoring of eq 13 for intermolecular exchange, as compared to mutual exchange, complete line shape calculations are possible only for relatively small spin systems. Our computer programs are presently restricted to systems with 45 or fewer allowed transitions for the observed nuclei.

Line Shape Calculations for the Basic Sets I–V

Figure 2 shows the NMR line shapes calculated for the $^{31}P\{^1H\}$ NMR spectrum of an HML_3^+-L system as a function of exchange rate using basic sets I and II. The high resolution NMR parameters used in this calculation were $\delta_1 = 1003$ Hz, $\delta_2 = \delta_3 = 639$ Hz, $\delta_4 = 2116$ Hz, $J_{12} = J_{13} = 31$ Hz. The effective transverse relaxation time T_2 was kept fixed at 0.075 sec for both HML_3^+ and L. Equimolar concentrations of HML_3^+ and L were assumed (these parameters correspond closely to those obtained from analyzing the 36.43-MHz $^{31}P\{^1H\}$ NMR spectra for the $HPd[P(C_2H_5)_3]_3^+$-$P(C_2H_5)_3$ system).[7] The line shape behavior associated with these two sets are readily distinguishable in practice, particularly at intermediate exchange rates (250-1250 sec^{-1}). The reason for the large difference in line shapes can be seen by referring to Figure 1. Basic set I exchanges only one of the two equivalent ligands L_2 and L_3 with L_1 or L_4 in a single permutation, whereas II exchanges both L_2 and L_3 with L_1 or L_4 during each permuta-
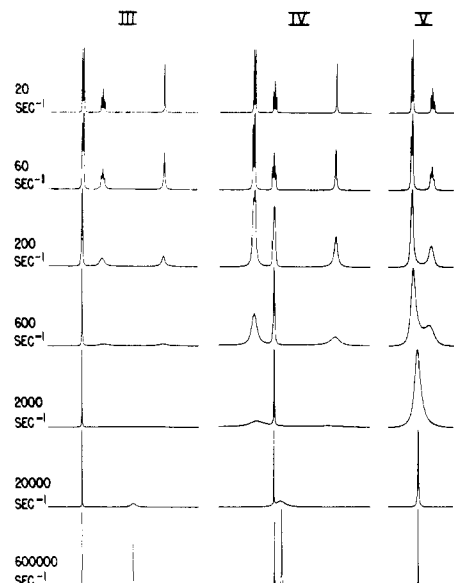
Figure 3. Line shape simulations for basic permutational sets III, IV, and V.
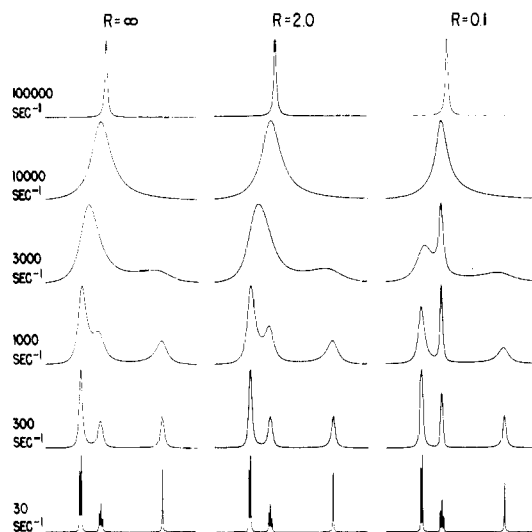

Figure 4. The effect of mutual exchange in the five-coordinate intermediate on the $^{31}P\{^1H\}$ NMR line shapes for an equimolar HML_3^+-L system. The exchange rate is the rate at which free ligand adds to HML_3^+. $R = \infty$ corresponds to very fast mutual exchange in the HML_4^+ intermediate. R is the ratio of the rate of mutual exchange to the rate of ligand dissociation in HML_4^+.

tion. Consequently, the resonances associated mainly with L_2 and L_3 are broader for set II at intermediate exchange rates (rates sufficiently fast to "decouple" the coupling of L_1 to L_2 and L_3 but slow enough that the chemical shift differences have not been averaged).

Figure 3 shows similar calculations for sets III, IV, and V. All three sets are qualitatively different from each other and from I and II. The free ligand resonance is not shown for set V since it is invariant to the exchange process. The remaining set (VI $\equiv$ E) corresponds to spectra invariant to both temperature and added ligand concentration.

The Effects of a Five-Coordinate Intermediate on the NMR Line Shapes

The presence of a five-coordinate intermediate of the type HML_4^+ can have two important effects on the NMR line shapes: (1) if the HML_4^+ cation is present in large enough concentrations, it must be included explicitly in the line shape calculations since the nuclear spins spend an appreciable fraction of their time at the HML_4^+ site; (2) if the preexchange lifetime for ligand dissociation is sufficiently long relative to the preexchange lifetime for mutual exchange, the HML_4^+ intermediate may rearrange before dissociation takes place.

Figures 4 and 5 show the effects of mutual exchange in the five-coordinate intermediate on the $^{31}P\{^1H\}$ NMR spectra for the intermolecular exchange process given by **2**. These line shapes were calculated using the linear combination of basic sets given by eq 2 and 8. The exchange rates given in these figures are the sums of the rates for each of the permutations corresponding to the linear combination of sets given in eq 2 including the identity set E. These rates are the rates at which the HML_3^+ species reacts with L to form HML_4^+.

The parameter R is equal to k_m/k_{-1}. The left-hand side of Figure 6 shows a similar calculation for an equimolar HML_3^+-L solution with the parameter R set at 0.5. The calculated spectra on the right-hand side of the figure were obtained by including the HML_4^+ resonances in the line shape calculation together with explicit account of the mutual exchange process using the equations of motion (11a–c).

The HML_4^+ cation was assumed to have a concentration 2.5% that of HML_3^+ and L. The high resolution NMR pa-
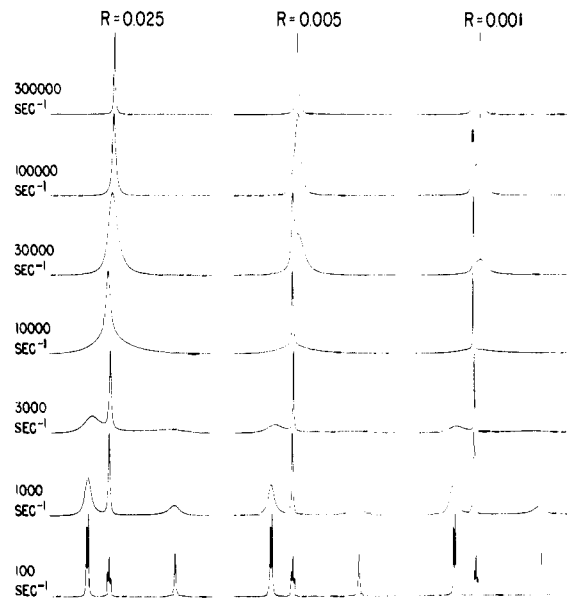

Figure 5. This figure is similar to Figure 4 except that the rate of mutual exchange in the HML_4^+ intermediate is slower.

rameters for the AB_3 spectrum corresponding to HML_4^+ were arbitrarily chosen as $J_{AB} = 40$ Hz, $\delta_A = 1203$ Hz, and $\delta_B = 839$ Hz. Since the group of the high resolution NMR Hamiltonian is not Abelian, the exchange matrix χ does have elements connecting transitions of zero and nonzero intensity. However, these connections were ignored in the line shape calculations. This procedure was checked by re peating the calculations with a slightly perturbed AB_3 sy tem shown in configuration **4** (the non-Abelian C_{3V} symm
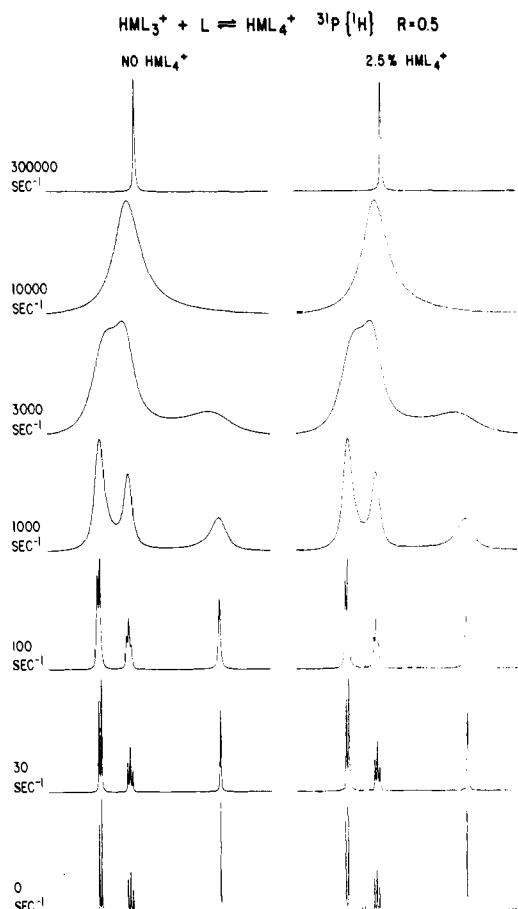

4
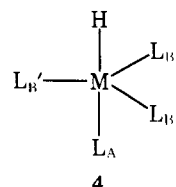
Figure 6. Comparison of two calculations of the NMR line shapes for an HML_3^+-HML_4^+-L system ($[HML_4^+] \to 0$). The calculations on the right-hand side explicitly include the HML_4^+ intermediate. The calculated spectra on the left do not include the HML_4^+ intermediate. This figure justifies the use of the linear combination of basic sets ($1 - C$) $(E + IV) + (C/3)(I + II + III + V)$ with the HML_3^+-L model to calculate NMR line shapes for the HML_3^+-L-HML_4^+ system ($[HML_4^+] \to 0$) in those cases where the HML_4^+ intermediate is stereochemically nonrigid. R is 0.5.

Figure 7. Effects of concentration, and NMR parameters of the HML_4^+ intermediate, on calculated NMR line shapes for an HML_3^+-HML_4^+-L system. The HML_4^+ intermediate is assumed to be rigid. The spectra on the left-hand side are almost identical with those that would be calculated using an HML_3^+-L model omitting the HML_4^+ resonances from the calculation.

try has been reduced to the Abelian C_s symmetry). The NMR parameters used in this calculation were $J_{AB} = 40$ Hz, $J_{AB'} = 40.1$ Hz, $\delta_A = 1203$ Hz, $\delta_B = 839$ Hz, $\delta_{B'} = 839.1$ Hz, and $J_{BB'} = 0.025$ Hz. The spectra shown on the two sides of Figure 6 are in very good agreement at all but the slowest exchange rates, thus demonstrating the validity of using the linear combination of basic sets given by eq 2 and 8 (provided $[HML_4^+]/[HML_3^+]$ is very small). The exchange rates given in Figure 6 and other figures in this paper are pseudo-first-order exchange rates for the HML_3^+ species. The corresponding pseudo-first-order exchange rates for HML_4^+ are, of course, much larger.

Figure 7 shows the effect of the HML_4^+ intermediate on the NMR line shapes calculated assuming that the intermediate is stereochemically rigid. For column A, $[HML_4^+]/[HML_3^+] = 0.01$. Except for spectra very near the slow exchange limit, the line shapes are almost identical with those calculated using the linear combination $E + IV$ for the HML_3^+-L model. The high resolution NMR parameters are the same as those used for Figure 6. In column B, the ratio $[HML_4^+]/[HML_3^+]$ has been increased to 0.1. In column C, $[HML_4^+]/[HML_3^+]$ is again 0.1, but the NMR parameters have been changed to $J_{AB} = 40$ Hz, $\delta_A = 1800$ Hz, and $\delta_B = 1950$ Hz. The combination of a fairly large $[HML_4^+]/[HML_3^+]$ ratio and the large frequency separation between the HML_3^+ and HML_4^+ resonances results in

a considerable difference between the spectra calculated using this model and those using the HML_3^+-L model.

Discussion

The rates of chemical processes under equilibrium conditions can be obtained from temperature dependent NMR line shapes. Activation energies of varying degrees of accuracy have been reported in a steadily increasing volume of publications.

More recently, efficient computational techniques have been developed to allow the calculation of line shapes in complex non-first-order spin systems undergoing *intramolecular* rearrangement.[1-4]

During the same period, group theoretical methods were applied to determine the extent of the *mechanistic* information contained in the exchange broadened spectra.[2,22]

The present paper has described the extension of both the general line shape calculations and the group theoretical mechanistic analyses to the mathematically more complicated situation in which *intramolecular* and *intermolecular* (bond breaking) processes are simultaneously involved. The example used[7,23] has been the case of a solution of $HPd[P(C_2H_5)_3]_3^+$ containing varying amounts of added $P(C_2H_5)_3$, assuming an equilibrium of the form

$$HPd[P(C_2H_5)_3]_3^+ + P(C_2H_5)_3 \underset{k_{-1}}{\overset{k_1}{\rightleftharpoons}} HPd[P(C_2H_5)_3]_4^+$$

(16)
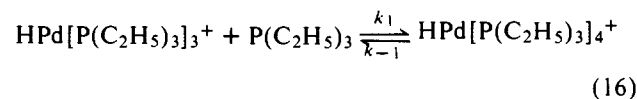
in which $HPdL_3^+$ is planar and rigid, $HPdL_4^+$ has C_{3v} symmetry with H on the C_3 axis, $HPdL_4^+$ is fluxional, and the free ligand participates in the simple associative process represented by eq 16.

In the most general case, for eq 16, four rate processes can be considered, k_1, k_{-1}, k_m (the rate of intramolecular rearrangement in HML_4^+), and k_m' (the rate of intramolecular rearrangement in HML_3^+); the latter process does not occur to a measurable extent in the $HPdL_3^+$ system.[7]
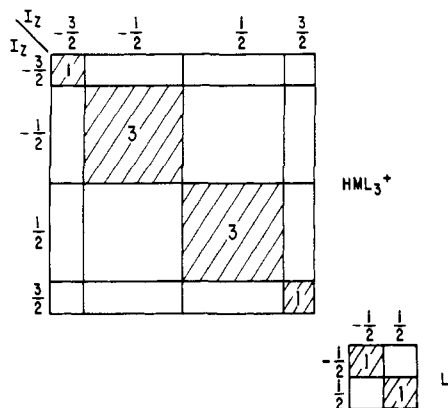
Figure 8. Structure of the spin Hamiltonians for the HML_3^+-L system. The nonzero parts of the matrices are shaded and their dimensions are indicated.
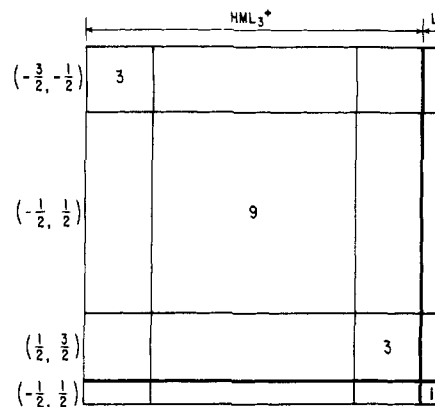

Figure 9. Structure of that part of the exchange matrix in χ connecting density matrix elements one off-diagonal in I_z. The I_z indices are indicated on the left-hand side and the species at the top. The total matrix is of dimension 16 × 16. Each of the 16 submatrices shown in the figure can be transformed separately since the total transformation matrix is block diagonal.

The computer programs have been written to handle all four rate processes. Application of the methods described in this paper to experimental data for a series of HML_3^+ complexes is presented in the following paper.[7]

The line shape calculations and the group theoretical analyses are not limited in application to the HML_3^+ systems; they are quite general, applicable to non-first-order systems, limited only by computer size and speed. As with the previous studies of intramolecular rearrangements, the calculations are based on a "jump" model and give no information concerning the actual details of the reaction coordinate. They simply provide information concerning the permutations which relate the nuclear labeling before exchange to the nuclear labeling after exchange. (This, however, is often sufficient to eliminate, unambiguously, many possible mechanisms.) In considering other physical mechanisms which are consistent with the permutational information, one must appeal to other chemical information to try to decide between them.

Specifically, for the HML_3^+ ($HPdL_3^+$) system we have shown that making the assumptions that (a) the exchange process is ligand catalyzed (an assumption clearly justified for the actual experimental situations),[7] and that (b) the process is concerted (this allows us to neglect for the moment the possibility of an intermediate of significant lifetime, such as HML_4^+, that can undergo intramolecular rearrangement), the permutational analysis of the HML_3^+ + L system shows that there are six distinguishable types of line shape behavior or "basic permutational sets" (I–VI) corresponding to the six possible exchanges shown in Figure 1.

Relaxing condition (a) above, i.e., explicitly considering an HML_4^+ intermediate, we have shown that (i) if HML_4^+ is present in very low concentrations and has a short preexchange lifetime, the effect of intramolecular rearrangement in HML_4^+ can be treated as an additional mechanism for permuting the free and complexed ligands by establishing the appropriate linear combination of "basic permutational sets". The resonances for HML_4^+ do not have to be included explicitly; (ii) if HML_4^+ is present in appreciable concentrations, it must be included explicitly in the calculations. Cases (i) and (ii) have been shown to converge as $[HML_4^+] \rightarrow 0$.

The general density matrix calculations have been described incorporating the k_1, k_{-1}, k_m, and k_m' rate processes (k_m' corresponds to intramolecular exchange in HML_3^+ discussed in more detail in the following paper).[7] Cases where the central metal M has an isotope with $I = \frac{1}{2}$ are considered.

The equations have been solved numerically to illustrate the line shape behavior for basic sets I-V in Figures 2 and 3 (set VI is the identity set). Qualitative comparison with the experimental spectra[7,23] shows immediately that only exchanges of type IV can predominate, this is particularly clear at low temperatures. Detailed line shape analyses can differentiate between all six cases corresponding to concerted processes.

Calculations using the appropriate linear combinations of basic sets to allow for intramolecular rearrangement in a transient HML_4^+ intermediate have been carried out (Figures 4 and 5). They show how the relative rates of intramolecular rearrangement and ligand dissociation $k_m/k_{-1} = R$ in HML_4^+ can be determined from the coefficients in the linear combination of basic sets used.

Additionally, complete calculations have been carried out in which the HML_4^+ resonances are included explicitly (Figure 6) and calculations in which HML_4^+ is assumed to be present in significant concentration and is stereochemically rigid are exemplified by Figure 7.

In summary, it is clear that nuclear resonance line shape studies of bond breaking processes at equilibrium can provide detailed mechanistic information, much of which would be unavailable using other approaches. Sites of ligand attack and the nature of rearrangement processes in intermediates and reactants can be determined in addition to conventional kinetic parameters. The methods are applied to a variety of systems in the succeeding paper.[7]

Appendix

Calculation Details. Transformation of the Density Matrix Equations of Motion. The structure of the effective high resolution NMR Hamiltonian used to calculate the $^{31}P\{^1H\}$ spectra for the HML_3^+-L systems ($I_M = 0$, $I_L = \frac{1}{2}$) is shown in Figure 8. The first step in the calculation is to set up the diagonal blocks of the spin Hamiltonians for each species involved in the exchange process and to diagonalize them numerically

$$T_{ij}^{-1} H_{ij} T_{ij} = \Lambda_{ij} \qquad (A1)$$

where H_{ij} is the jth block, diagonal in I_z, of the spin-Hamiltonian for the ith species. T_{ij} is the corresponding transformation matrix and Λ_{ij} is diagonal. The transition matrices $M^-_{i(j,j+1)}$, one off-diagonal in I_z, are then set up in the original basis of simple products of the eigenvectors of I_z for the individual spins, and transformed to the new basis:

$$M'^{-}_{i(j,j+1)} = T_{ij}^{-1}M^{-}_{i(j,j+1)}T_{i(j+1)} \qquad (A2)$$

The program then searches for the nonzero elements of the $M'^{-}_{i(j,j+1)}$ corresponding to allowed transitions, and indices indicating their location are stored. Typically, elements of the M^{-} with values greater than 10^{-4} are considered to correspond to allowed transitions.

Figure 9 shows the structure of the exchange matrix in Liouville space, connecting the spin density matrix elements for HML_3^+ and L, which are one off diagonal in I_z. In general, all the elements of this matrix may be nonzero. The procedure used for transforming the exchange matrix χ is to set up each of the submatrices $\chi_{ij:kl}$ in turn, where $\chi_{ij:kl}$ is that part of χ connecting $\rho_{i(j,j+1)}$ and $\rho_{k(l,l+1)}$ in the equation of motions. $\rho_{i(j,j+1)}$ is that part of the density vector in Liouville space for species i corresponding to the density matrix elements one off diagonal in I_z between $I_z = j$ and $I_z = j + 1$. In general, there are $(\Sigma_i N_i)^2$ such submatrices where N_i is the number of spins (of $\frac{1}{2}$) for the ith species. The appropriate transformation for each of these submatrices is given by

$$\chi'_{ij:kl} = (T_{ij} \otimes T_{i(j+1)})^{-1} \quad \chi_{ij:kl} \ (T_{kl} \otimes T_{k(l+1)}) \quad (A3)$$

After the transformation has been carried out, the elements of $\chi'_{ij:kl}$ connecting density matrix elements corresponding to allowed transitions are stored.

The reason for this procedure is to avoid having to store all the elements of χ connecting density matrix elements one off diagonal in I_z. For the HML_3^+-L problem ($^{31}P\{^1H\}$), these elements could be stored in a 16 × 16 matrix (Figure 9) and no core storage problems would arise. However, for the HML_4^+-HML_3^+-L calculations a 72 × 72 matrix would be required which must then be transformed. Using the procedure outlined above the largest submatrix of χ which must be transformed is of order 24 × 24 for the HML_4^+-HML_3^+-L calculations and 9 × 9 (Figure 9) for the HML_3^+-L calculations.

The transformation allows the order of the complex non-Hermitian matrix, which must be diagonalized to calculate the NMR line shapes, to be reduced from 16 × 16 to 10 × 10 for the HML_3^+-L ($^{31}P\{^1H\}$) calculations, from 72 × 72 to 44 × 44 for the C_s HML_4^+-HML_3^+-L problem, and from 72 × 72 to 34 × 34 for the C_{3v} HML_4^+-HML_3^+-L problem. The transformation improves the numerical stability as well as reducing the core storage and computer time requirements for the calculation.

References and Notes

(1) G. Binsch, *J. Am. Chem. Soc.*, **91**, 1304 (1969).
(2) P. Meakin, E. L. Muetterties, F. N. Tebbe, and J. P. Jesson, *J. Am. Chem. Soc.*, **93**, 4701 (1971).
(3) J. M. Krieger, J. M. Deutch, and G. M. Whitesides, *Inorg. Chem.*, **12**, 1535 (1973).
(4) J. M. Gilles, Thesis Universite Libre de Bruxelles, 1969.
(5) J. P. Fackler, Jr., J. A. Fetchin, J. Mayhew, W. C. Seidel, T. J. Swift, and M. Weeks, *J. Am. Chem. Soc.*, **91**, 1941 (1969).
(6) O. Yamamoto and N. Kamezawa, *J. Magn. Reson.*, **3**, 269 (1970).
(7) Analysis of experimental data for the HML_3^+ ligand association reactions is presented in part II of this series: A. D. English, P. Meakin, and J. P. Jesson, *J. Am. Chem. Soc.*, following paper in this issue.
(8) J. P. Jesson and P. Meakin, *Acc. Chem. Res.*, **6**, 269 (1973).
(9) W. G. Klemperer in "Dynamic Nuclear Magnetic Resonance Spectroscopy", F. A. Cotton and L. M. Jackman, Ed., Academic Press, New York, N.Y., 1974.
(10) W. G. Klemperer, J. K. Krieger, M. D. McCreary, E. L. Muetterties, D. O. Traficante, and G. M. Whitesides (submitted for publication).
(11) Here and in subsequent parts of this paper I will be used to represent the combination I + IA of basic sets.
(12) A. D. English, P. Meakin, and J. P. Jesson (submitted for publication).
(13) The linear combination (E + IV) of basic sets is used rather than IV alone because dissociation of the ligand L_4, which was not coordinated to M in the HML_3^+ cation, will lead to no permutation of free and complexed ligands (set E). However, this process, which does not contribute to the NMR line shapes, must be included in calculating the total rate of the process $HML_3^+ + L \rightleftharpoons HML_4^+$. The notation (E + IV) indicates that the permutation in the sets E and IV are included in the calculations with the same exchange rate. Similarly, the notation A(E + IV) + B(I + II + III + V) indicates that the three permutations in (E + IV) are included with the same rate, and the seven permutations in (I + II + III + V) are included with the same rate. The relative rates for the permutations in (E + IV) with respect to those in (I + II + III + V) is A/B.
(14) J. I. Kaplan, *J. Chem. Phys.*, **28**, 278 (1958); **29**, 462 (1958).
(15) S. Alexander, *J. Chem. Phys.*, **37**, 974 (1962).
(16) J. I. Kaplan and G. Fraenkel, *J. Am. Chem. Soc.*, **94**, 2907 (1972).
(17) P. Meakin and J. P. Jesson, *J. Am. Chem. Soc.*, **95**, 7272 (1973).
(18) J. P. Jesson and P. Meakin, *J. Am. Chem. Soc.*, **96**, 5760 (1973).
(19) Boldface type is used to denote vectors, matrices, and operators (superoperators) in Liouville space.
(20) R. G. Gordon and R. P. McGinnis, *J. Chem. Phys.*, **49**, 2455 (1968).
(21) R. E. Schirmer, J. H. Noggle, and D. F. Gaines, *J. Am. Chem. Soc.*, **91**, 6240 (1969).
(22) W. G. Klemperer, *J. Chem. Phys.*, **56**, 5478 (1972).
(23) P. Meakin, R. A. Schunn, and J. P. Jesson, *J. Am. Chem. Soc.*, **96**, 277 (1974).